Eur. Phys. J. C 49, 321–326 (2007)
DOI 10.1140/epjc/s10052-006-0086-5

THE EUROPEAN PHYSICAL JOURNAL C

Regular Article – Experimental Physics

What can we learn from high-p_{T} correlations of neutral strange baryons and mesons at RHIC?

J. Bielcikova[a] for the STAR Collaboration

Physics Department, Yale University, P.O. Box 208120, New Haven, CT 06520-8120, USA

Received: 11 August 2006 /
Published online: 28 November 2006 –

Abstract. We present results on two-particle azimuthal correlations of neutral strange baryons (Λ, $\overline{\Lambda}$) and mesons (K^0_S) for $p_{\mathrm{T}} = 2$–$6\,\mathrm{GeV}/c$ associated with non-identified charged particles in $d+\mathrm{Au}$ and $\mathrm{Au}+\mathrm{Au}$ collisions at $\sqrt{s_{NN}} = 200\,\mathrm{GeV}$ measured by the STAR experiment. We investigate in detail the associated yield of charged particles as a function centrality of the collision and transverse momentum of trigger and associated particles to look for possible flavor, baryon/meson and particle/anti-particle differences. We compare our results to the proton and pion triggered correlations as well as to a fragmentation and recombination model.

PACS. 25.75.-q; 25.75.Gz

1 Introduction

Partonic energy loss has been predicted to be a sensitive probe of the matter created in high energy heavy-ion collisions because its magnitude depends strongly on the color charge density of the medium traversed [1–3]. Partons originating from hard scattering of quarks or gluons from the two colliding nuclei fragment into jets. As a direct measurement of jets in heavy-ion collisions is difficult due to the large number of produced particles, azimuthal correlations of particles with large transverse momentum (p_{T}) are conventionally used to study jet related processes.

Studies of azimuthal correlations of charged particles in central $\mathrm{Au}+\mathrm{Au}$ collisions at RHIC resulted in several interesting observations which show striking differences to p+p and $d+\mathrm{Au}$ measurements: (i) *disappearance* of the away-side jet at intermediate p_{T} [4], (ii) *re-appearance* of the away-side yield in the increased production of low p_{T} particles [5], (iii) *punch through* or observations of di-jets with sufficiently large p_{T} to traverse the hot and dense medium [6], and (iv) presence of long range pseudo-rapidity ($\Delta\eta$) correlations on the near side [7].

In addition, measurements of the suppression of inclusive p_{T} spectra of identified particles in central $\mathrm{Au}+\mathrm{Au}$ collisions with respect to $p+p$ collisions (R_{AA}) and peripheral $\mathrm{Au}+\mathrm{Au}$ collisions (R_{CP}) [8, 9] together with *enhanced baryon/meson ratios* [10] show that in the intermediate p_{T} range of 2–6 GeV/c at RHIC energies baryons and mesons behave differently than in $p+p$ collisions. This indicates that jet fragmentation is not a dominant source of particle production and parton recombination and coalescence models have been suggested as an alternative mechanism [11–15].

Identified two-particle correlations are expected to provide additional information on jet quenching, the origin of long range $\Delta\eta$ correlations, the baryon–meson puzzle and particle production mechanisms at RHIC energies in general. In this paper, we present results on identified strange baryon (Λ, $\bar{\Lambda}$) and meson (K^0_S) triggered correlations in the intermediate p_{T} range in $d+\mathrm{Au}$ and $\mathrm{Au}+\mathrm{Au}$ collisions at $\sqrt{s_{NN}} = 200\,\mathrm{GeV}$ measured by the STAR experiment.

2 STAR experiment

STAR is a large acceptance, multi-purpose spectrometer consisting of several detectors inside a large solenoidal magnet with a magnetic field of 0.5 T. Our analysis is based exclusively on charged particle tracks detected and reconstructed in the Time Projection Chamber (TPC). The TPC is especially well suited for the correlation studies because of its full azimuthal coverage and pseudo-rapidity acceptance $|\eta| < 1.8$. The TPC provides up to 45 independent spatial and energy loss ($\mathrm{d}E/\mathrm{d}x$) measurements along each charged particle track. The momentum resolution is determined to be $\Delta k/k \sim 0.0078 + 0.0098 p_{\mathrm{T}}\,(\mathrm{GeV}/c)$ [16].

The weakly decaying strange particles (V0s) can be reconstructed by a topological analysis from their decay products measured in the TPC. Λ, $\bar{\Lambda}$ and K^0_S particles used in our study were reconstructed via the following decay channels:

$$\Lambda \to p + \pi^-\,, \qquad \mathrm{BR} = (63.9 \pm 0.5)\%\,,$$

[a] e-mail: jana.bielcikova@yale.edu

$$\bar{\Lambda} \to \bar{p} + \pi^+ , \qquad \mathrm{BR} = (63.9 \pm 0.5)\% ,$$
$$K^0_S \to \pi^+ + \pi^- , \qquad \mathrm{BR} = (68.95 \pm 0.14)\% . \quad (1)$$

The geometrical cuts have been optimized to achieve a very clean sample of the V0 particles. Above $p_T > 2\,\mathrm{GeV}/c$ the signal to background ratio with these cuts is approximately 15 : 1.

The results presented in this paper are based on the $d+\mathrm{Au}$ data set taken in 2003 and $\mathrm{Au}+\mathrm{Au}$ data set measured in 2004 at $\sqrt{s_{NN}} = 200$ GeV.

3 Two-particle correlations

In the azimuthal correlations presented here, we distinguish several trigger particle species (charged particles, Λ, $\bar{\Lambda}$, and K^0_S), while the associated particles are always charged particles. The azimuthal distributions are then defined as

$$D(\Delta\varphi) = \frac{1}{N_{\mathrm{trigger}}} \frac{1}{\varepsilon} \int \mathrm{d}(\Delta\eta) N(\Delta\varphi, \Delta\eta) , \quad (2)$$

where $\Delta\varphi = \varphi^{\mathrm{trigger}} - \varphi^{\mathrm{associated}}$ is the azimuthal angle difference between the trigger and the associated particle, N_{trigger} is the number of trigger particles, and ε is the reconstruction efficiency of associated charged particles.

The measured azimuthal distributions are normalized to the number of trigger particles and corrected for the reconstruction efficiency of associated charged particles which, in the p_T range studied, varies from 70% to 84% depending on centrality. The data are fit with two Gaussians on top of a flat background in $d+\mathrm{Au}$ and elliptic flow modulated background in $\mathrm{Au}+\mathrm{Au}$ collisions, respectively. We use two methods to adjust the level of the elliptic flow modulated background: a free parameter fit and the ZYAM (zero yield at minimum) method [17]. For the latter one in order to avoid problems from statistical fluctuations the level of the elliptic flow modulated background is determined as an average from several (typically 3 to 5) neighbouring bins in the "valley region". The yield values obtained by the ZYAM procedure are about 15% higher than those obtained from fitting the level of the background. This, together with uncertainties in the v_2 values, results in a systematic error of about 30% on the extracted associated yield values on the near side.

Figure 1 shows a comparison of strange baryon/meson (left) and baryon/anti-baryon (right) triggered correlation functions in central (0–5%) and semi-central (30–40%) $\mathrm{Au}+\mathrm{Au}$ collisions after the subtraction of the elliptic flow modulated background and for $|\eta| < 1$. The transverse momentum selection is $p_T^{\mathrm{trigger}} = 3.0$–$3.5\,\mathrm{GeV}/c$ for the trigger, and $p_T^{\mathrm{associated}} = 1$–$2\,\mathrm{GeV}/c$ for the associated particles.

In order to separate the jet (J) contribution on the near side from long-range pseudo-rapidity correlations (commonly referred to as the *ridge*, R), we analyze the azimuthal correlations in two different $\Delta\eta$ windows: $\Delta\eta < 0.5$ which includes contributions from both jet and ridge, and

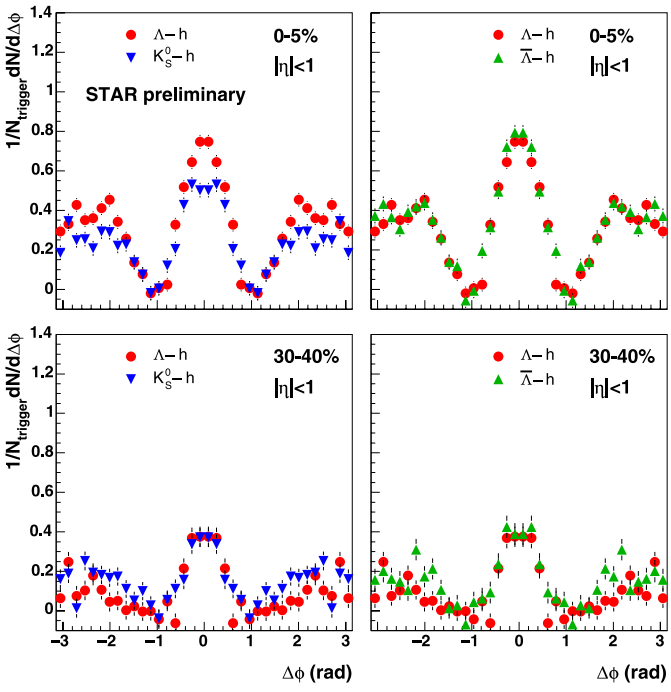

Fig. 1. Two-particle azimuthal correlations for various trigger species: Λ and K^0_S triggered correlations (*left column*) and Λ and $\bar{\Lambda}$ triggered correlations (*right column*) in central (0–5%) (*top*) and semi-central (30–40%) (*bottom*) $\mathrm{Au}+\mathrm{Au}$ collisions at $\sqrt{s_{NN}} = 200$ GeV. The elliptic flow contribution has been subtracted using the ZYAM method. The trigger particles are selected with $3.0 < p_T^{\mathrm{trigger}} < 3.5\,\mathrm{GeV}/c$, the associated charged particles with $1 < p_T^{\mathrm{associated}} < 2\,\mathrm{GeV}/c$

$\Delta\eta > 0.5$ influenced only by the long-range $\Delta\eta$ correlations. Subtracting the two removes both the elliptic flow and ridge (under the assumption that the v_2 and ridge contributions are constant in η). What remains are jet-like correlations [7].

4 Results

Below, we discuss in detail the properties of the near-side yield of associated charged particles which is calculated as the area under the Gaussian peak obtained from the fit to the correlation functions. In particular, the near-side yield is studied as a function of system size, centrality and the transverse momentum of the trigger and the associated particles.

4.1 System size dependence

Figure 2 shows the near-side associated yield of charged particles with $p_T = 1$–$2\,\mathrm{GeV}/c$ as a function of the transverse momentum of the trigger particle, p_T^{trigger} for various trigger species in $d+\mathrm{Au}$ and in central $\mathrm{Au}+\mathrm{Au}$ collisions. To look for possible baryon/meson differences, we have included in Fig. 2b the results for π^+ and π^- (95% purity) as well as p and $\bar{p}$ (50% purity) trigger particles which were

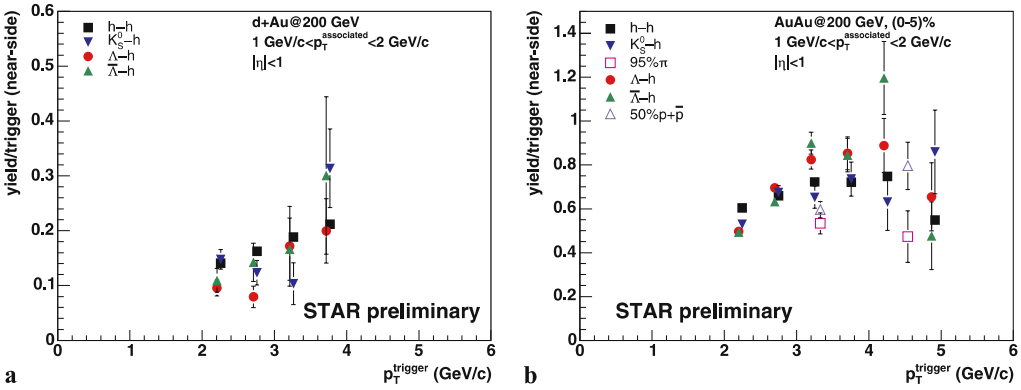

Fig. 2. Near-side associated charged particle yield as a function of $p_{\mathrm{T}}^{\mathrm{trigger}}$ in $d+$Au **a** and central Au + Au collisions **b** at $\sqrt{s_{NN}} = 200$ GeV. Various trigger particle species are indicated by the legend. The data points for baryons are offseted by 50 MeV/c for a better view. The errors are statistical only

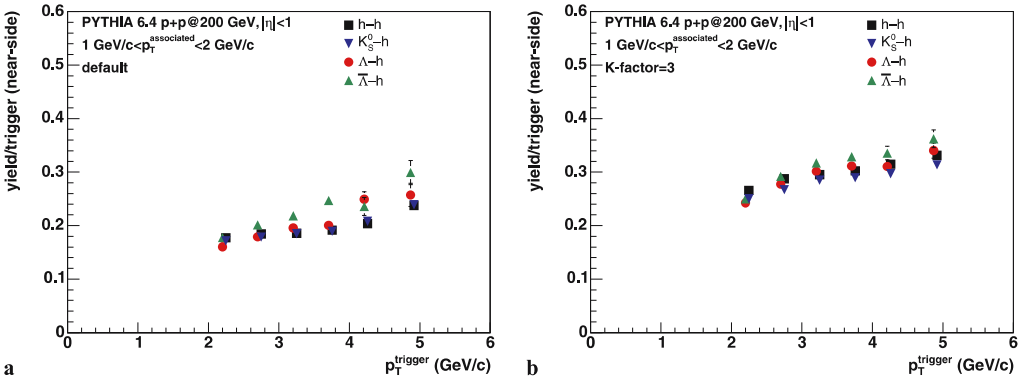

Fig. 3. Near-side associated charged particle yield as a function of $p_{\mathrm{T}}^{\mathrm{trigger}}$ in default **a** and using K-factor = 3 **b** PYTHIA simulation of $p+p$ at $\sqrt{s_{NN}} = 200$ GeV. Various trigger particle species are indicated by the *legend*

identified by the relativistic rise of the specific ionization energy loss ($\mathrm{d}E/\mathrm{d}x$) in the TPC [18]. There are no significant differences between the trigger species within the statistical errors in either collision system.

Assuming the near-side jet yields measured in $d+$Au collisions are close to those in $p+p$ collisions [19] (which we do not have available), we compare them to PYTHIA [20], a leading order pQCD model. To make this comparison, we have used PYTHIA 6.4. The results on the near-side yield of associated charged particles are shown in Fig. 3. Figure 3a corresponds to the default PYTHIA setting which it is known does not describe well the inclusive p_{T} spectra of strange particles (e.g. Λ, K^0_S, Ξ^-) [21]. However, the jet yield values are in a good agreement with those measured in $d+$Au collisions. Regarding the species dependence, all trigger species apart from the $\bar{\Lambda}$ behave similarly, with the $\bar{\Lambda}$ being systematically higher. In order to describe the p_{T} distributions of strange particles, a K-factor is commonly introduced which simulates the next-to-leading order contributions and changes the mixture of $q+q$, $q+g$ and $g+g$ processes. We have chosen a K-factor of 3 which has been successful in describing the strange particle spectra, and calculated the corresponding near-side jet yields. The results are plotted in Fig. 3b. As we can see, the $\bar{\Lambda}$ yields are the same as for the charged and Λ triggered correlations which is due to the fact that the mixture of the parton-parton processes favors those involving gluons. But the associated yield is now 50% higher and thus in disagreement with our measurements. This has to do with the fact that too many pions are generated with the K-factor = 3. To summarize, the default PYTHIA calculation offers a satisfactory description of jet yields but fails to describe inclusive p_{T} spectra of strange particles, while PYTHIA with the K-factor = 3 describes the inclusive p_{T} strange particle spectra well but fails to reproduce the jet yield values. Thus a more sophisticated tuning of PYTHIA is required in order to describe both, p_{T} spectra and two-particle correlations at the same time.

Comparing the values of the near-side yields in $d+$Au and Au + Au collisions, we observe a clear difference between the two systems. The yield in central Au + Au collisions is about 3–4 times larger than in $d+$Au collisions, independent of the trigger species and $p_{\mathrm{T}}^{\mathrm{trigger}}$. The large increase in the yield of associated particles in Au + Au collisions can be understood in the framework of the recombination model [22]. This calculation shows that in Au + Au collisions, a thermal-shower recombination plays a dominant role while it is much less prominent in the $d+$Au system. Although the calculation has been done for charged pions while we measure correlations of identified-strange hadrons with unidentified-charged particles, the qualitative features of the data are well reproduced by the recombination model.

4.2 Centrality dependence

Next, we discuss the centrality dependence of the near-side yield of associated charged particles. The trigger particles are selected with $p_{\mathrm{T}}^{\mathrm{trigger}} = 3$–$6$ GeV/c and the associated charged particles have to satisfy the condition $1.5\,\mathrm{GeV}/c < p_{\mathrm{T}}^{\mathrm{associated}} < p_{\mathrm{T}}^{\mathrm{trigger}}$. Please note, that in the

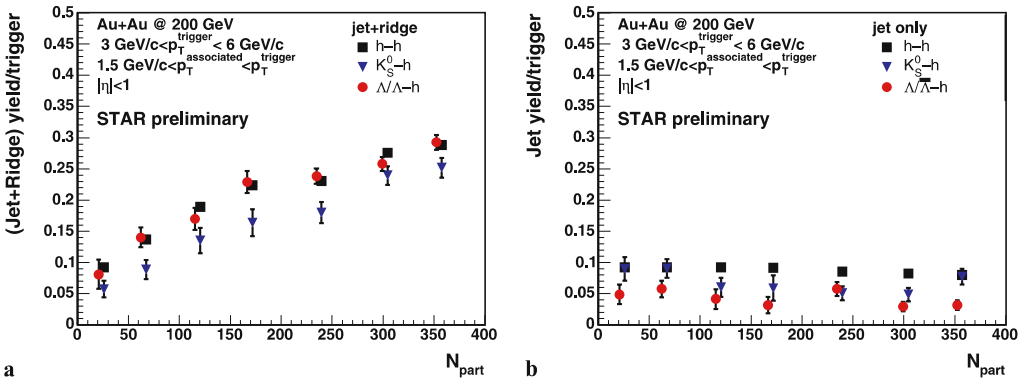

Fig. 4. Near-side associated charged particle yield as a function of centrality in Au + Au collisions: jet+ridge, $J + R$ **a** and jet only, J **b**. Transverse momentum of trigger particles is $p_T^{trigger} = 3$–6 GeV/c and various trigger species are described by the legend. The errors are statistical only

centrality study, we have increased the lower threshold on the transverse momentum of associated particles in order to be able to separate the jet (J) contribution from the ridge (R) contribution. The near-side yield within the full $\Delta\eta$ acceptance and after the elliptic flow subtraction is plotted in Fig. 4a as a function of the number of participants, N_{part}. The yield increases by a factor of 3–4 from peripheral to central Au + Au collisions for all trigger species studied. The observed increase between peripheral and central Au + Au collisions is consistent with the increase observed between d + Au to central Au + Au collisions (see Fig. 2 and Sect. 4.1). The $J + R$ yield for K_S^0 triggered correlations is systematically below that of charged and Λ triggered correlations. However, taking into account the statistical errors and systematic uncertainities dominated by the elliptic flow subtraction, the observed difference is not significant.

Calculating the azimuthal correlations in two different $\Delta\eta$ windows: $\Delta\eta < 0.5$ and $\Delta\eta > 0.5$, we have extracted the jet yield as a function of centrality. The results plotted in Fig. 4b demonstrate the independence of the jet yield on the centrality of the collision. The determination of the jet yield is not hampered by the large systematic errors on the elliptic flow subtraction as the elliptic flow is automatically removed by subtracting two different $\Delta\eta$ windows, assuming that the v_2 is uniform within the STAR acceptance. Within statistical errors, there is no significant dependence on the trigger species, although the jet yield for Λ and K_S^0 triggers is systematically below that of charged trigger particles. There are two effects which can possibly explain this difference. The artificially merged tracks in the TPC, which is a purely instrumental effect, may result in a lower associated yield because for the same p_T the track merging affects more the V0s than the charged particles [23]. The second reason, which has to do with physics, could be linked to the fact that baryon triggered jet takes away more energy than the meson triggered one (as the baryon is more massive than the meson). Therefore, less energy is available for the associated particle production. Both effects are currently under investigation.

From the comparison of both Fig. 4a and b, we can see that the ridge yield, R, is responsible for the strong increase of the near-side associated yield with centrality. While it is negligible in the peripheral Au + Au collisions, in central Au + Au collisions the ridge yield accounts for about 2/3 of the associated yield at near-side in the studied p_T range.

4.3 Transverse momentum dependence of associated particles

Figure 5 shows an example of the invariant transverse momentum distribution of associated charged particles on the near side in the 0–10% most central Au + Au collisions. Here, we have again selected the trigger particles with $p_T^{trigger} = 3$–6 GeV/c. The figure contains two sets of data points: the $p_T^{associated}$ spectra for $J + R$ yield and J yield only. Clearly, the $J + R$ spectrum is softer than the corresponding spectrum for jet-like correlations. To quantify the difference, we have fit the data with an exponential function ($Ae^{-p_T/T}$) and extracted the inverse slope values, T,

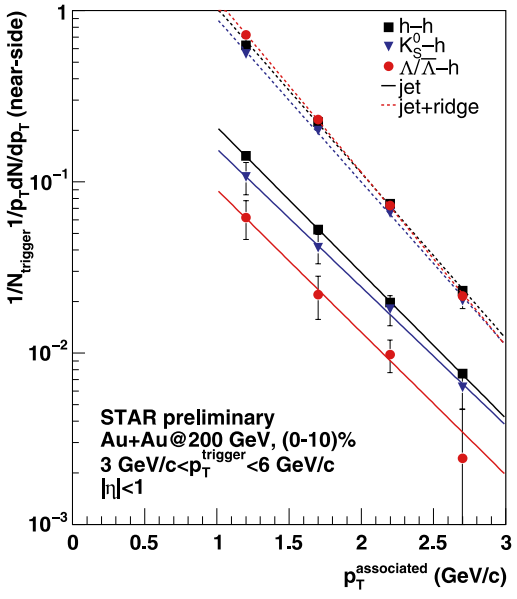

Fig. 5. Invariant transverse momentum distributions of associated charged particles on the near-side in central (0–10%) Au + Au collisions for various trigger species indicated by the legend. The *lines* are exponential fits to the data: jet + ridge (*dashed*) and jet only (*solid*). Transverse momentum of trigger particles is $p_T^{trigger} = 3$–6 GeV/c. The errors are statistical only

Table 1. Inverse slope, T, values of J and $J+R$ near-side associated charged particle p_T distributions for various trigger species with $p_T^{trigger} = 3$–6 GeV/c. The T values are calculated for 0–10% central Au + Au collisions

Trigger	$T(J)$ MeV	$T(J+R)$ MeV
h	511 ± 6	450 ± 3
K^0_S	539 ± 58	456 ± 13
Λ	522 ± 84	430 ± 8

which are summarized in Table 1. The extracted inverse slope values for various trigger species overlap within the statistical errors. The inverse slope of the jet spectrum is $T(J) \sim 510$–540 MeV, which is on average approximately 80 MeV harder than that of the total near-side associated yield $T(J+R) \sim 430$–450 MeV.

In order to make a comparison with a parton recombination model, we have extracted the $p_T^{associated}$ spectra in the $J+R$ case in peripheral 40–80% Au + Au collisions and calculated their central-to-peripheral ratio. The results are depicted in Fig. 6 together with the ratio calculated from the recombination model [22]. The ratio decreases from about 3 at $p_T^{associated} = 1$ GeV/c to 2 at $p_T^{associated} = 3$ GeV/c. Again, there is a hint of a trend of a baryon/meson splitting although within the statistical and systematic errors the splitting is not significant.

The observed decrease of the central-to-peripheral ratio with $p_T^{associated}$, as well as the large magnitude of the ratio, is in line with the model expectations and points toward a significant role of thermal-shower recombination in Au + Au collisions [22]. We remark here, that the calculation has not been done with exactly the same selection

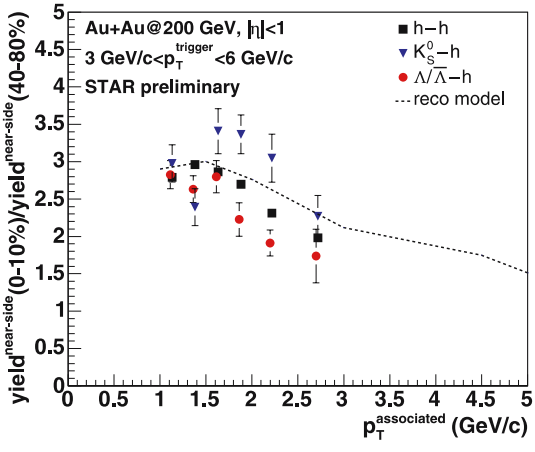

Fig. 6. The ratio of the near-side associated charged particle yield in central (0–10%) and peripheral (40–80%) Au + Au collisions as a function of $p_T^{associated}$. The transverse momentum of trigger particles is $p_T^{trigger} = 3$–6 GeV/c and various trigger species are described by the legend. The *dashed line* is taken from [22] and represents the central-to-peripheral ratio for $p_T^{trigger} = 4$–6 GeV/c and centrality (0–10%)/(80–92%). The errors are statistical only

criteria as our analysis. Firstly, there is a slightly different $p_T^{trigger}$ selection ($p_T^{trigger} = 4$–6 GeV/c), but the authors of [22] have shown that there is only a very small dependence on $p_T^{trigger}$. More importantly, there is a difference in the centrality selection for the peripheral collisions. The model prediction has been calculated for 80–92% centrality, while our most peripheral data were measured only up to 80% of the geometrical cross section. Last, but not least, the model uses as trigger particles charged pions and calculates only the yield of charged pions, while we use charged, Λ, K^0_S trigger particles and charged associated particles. The last two selections need to be adjusted in the model to our data in order to draw a quantitative conlusion on the agreement with the recombination model. In addition, as long range pseudo-rapidity correlations play a significant role in Au + Au collisions in the studied p_T range, a check of how well they are reproduced in the model is also required.

5 Conclusions

We have reported results on the near-side associated yield of charged particles for charged hadron and neutral strange baryon (Λ, $\bar{\Lambda}$) and meson (K^0_S) trigger particles in d + Au and Au + Au collisions at $\sqrt{s_{NN}} = 200$ GeV. In the transverse momentum range $p_T = 2$–6 GeV/c, we do not observe any appreciable baryon/meson or particle/antiparticle differences in either collision system.

The observed large increase by a factor 3–4 of the near-side yield from d + Au towards central Au + Au collisions can be qualitatively understood in the framework of parton recombination due to a dominant contribution from thermal-shower recombination in Au + Au collisions. A quantitative comparison requires the same p_T and centrality selections as in the data.

Based on the centrality dependence of the near-side yield and p_T spectra of associated charged particles, we have established the existence of long range pseudo-rapidity correlations (the 'ridge') for Λ and K^0_S previously observed for unidentified charged particles [7]. In the p_T range studied here the jet/ridge ratio is about 1/3. The spectra of associated particles in the jet are harder by ~ 80 MeV than those from the ridge. There are several models which attempt to explain the origin of the ridge: the coupling of parton radiation to longitudinal flow [24], parton recombination [25], or a combination of jet quenching and radial flow [26]. However, there are no quantitative predictions available yet. Ongoing studies with larger statistics using identified associated particles (π, p, Λ, K^0_S) will help to constrain the origin of the long-range pseudo-rapidity correlations.

Acknowledgements. We thank the RHIC Operations Group and RCF at BNL, and the NERSC Center at LBNL for their support. This work was supported in part by the Offices of NP and HEP within the U.S. DOE Office of Science; the U.S. NSF; the BMBF of Germany; CNRS/IN2P3, RA, RPL, and EMN of France; EPSRC of the United Kingdom; FAPESP of Brazil; the

Russian Ministry of Science and Technology; the Ministry of Education and the NNSFC of China; IRP and GA of the Czech Republic, FOM of the Netherlands, DAE, DST, and CSIR of the Government of India; Swiss NSF; the Polish State Committee for Scientific Research; SRDA of Slovakia, and the Korea Sci. and Eng. Foundation.

References

1. M. Gyulassy, M. Plumer, Phys. Lett. B **243**, 432 (1990)
2. X.-N. Wang, M. Gyulassy, Phys. Rev. Lett. **68**, 1480 (1992)
3. R. Baier, D. Schiff, B.G. Zakharov, Ann. Rev. Nucl. Part. Sci. **50**, 37 (2000)
4. C. Adler et al., Phys. Rev. Lett. **90**, 082 302 (2003)
5. J. Adams et al., Phys. Rev. Lett. **95**, 152 301 (2005)
6. J. Adams et al., nucl-ex/0604018
7. J. Putschke, Proc. Hot Quarks 2006
8. S. S. Adler et al., Phys. Rev. Lett. **91**, 172 301 (2003)
9. J. Adams et al., Phys. Rev. Lett. **92**, 052 302 (2004)
10. J. Adams et al., nucl-ex/0601042
11. R.J. Fries, B. Muller, C. Nonaka, S.A. Bass, Phys. Rev. C **68**, 044 902 (2003)
12. I. Vitev, M. Gyulassy, Phys. Rev. C **65**, 041 902 (2002)
13. V. Greco, C.M. Ko, P. Levai, Phys. Rev. C **68**, 034 904 (2003)
14. V. Greco, C.M. Ko, P. Levai, Phys. Rev. Lett. **90**, 202 302 (2003)
15. R.C. Hwa, C.B. Yang, Phys. Rev. C **67**, 034 902 (2003)
16. M. Anderson et al., Nucl. Instrum. Methods A **499**, 659 (2003)
17. N.N. Ajitanand et al., Phys. Rev. C **72**, 011 902 (2005)
18. J.G. Ulery, nucl-ex/0510055 (2005)
19. J. Adams et al., Phys. Rev. Lett. **91**, 072 304 (2003)
20. T. Sjostrand, S. Mrenna, P. Skands, JHEP **05**, 026 (2006)
21. M. Heinz, hep-ex/0606020
22. R.C. Hwa, Z. Tan, Phys. Rev. C **72**, 057 902 (2005)
23. L. Gaillard, Proc. Hot Quarks 2006
24. N. Armesto, C.A. Salgado, U.A. Wiedemann, Phys. Rev. Lett. **93**, 242 301 (2004)
25. C.B. Chiu, R.C. Hwa, Phys. Rev. C **72**, 034 903 (2005)
26. S.A. Voloshin, Nucl. Phys. A **749**, 287 (2005)